Fibroblast activation protein imaging in atrial fibrillation: a proof-of-concept study

Lina Li
Beijing Chaoyang Hospital
Jie Gao
Beijing Chaoyang Hospital
Bi-Xi Chen
Beijing Chaoyang Hospital
Xingpeng Liu
Beijing Chaoyang Hospital
Liang Shi
Beijing Chao-Yang Hospital Capital Medical University: Beijing Chaoyang Hospital
Yanjiang Wang
Beijing Chao-Yang Hospital Capital Medical University: Beijing Chaoyang Hospital
Li Wang
Beijing Chao-Yang Hospital Capital Medical University: Beijing Chaoyang Hospital
Pixiong Su
Beijing Chao-Yang Hospital Capital Medical University: Beijing Chaoyang Hospital
Min-Fu Yang
Beijing Chao-Yang Hospital Capital Medical University: Beijing Chaoyang Hospital
https://orcid.org/0000-0002-9015-0541
Boqia Xie (dr.boqiaxie@hotmail.com)
Beijing Chaoyang Hospital https://orcid.org/0000-0003-4490-9032

Research Article

Keywords: Fibroblast activation protein inhibitor; atrial fibrillation; atrial fibrosis; fibroblast

Posted Date: August 9th, 2022

DOI: https://doi.org/10.21203/rs.3.rs-1917675/v1

Fibroblast activation protein imaging in atrial fibrillation: a proof-of-concept study

Lina Li[1*] MD, Jie Gao[2*] MD, Bi-Xi Chen[1*] MD, Xingpeng Liu[2] MD, Liang Shi[2] MD, Yanjiang Wang[2] MD, Li Wang[1] MD, Pixiong Su[2] MD, Min-Fu Yang[1] MD, Boqia Xie[2] MD

[1] Department of Nuclear Medicine, Beijing Chaoyang Hospital, Capital Medical University, Beijing, China

[2] Cardiac Center, Beijing Chaoyang Hospital, Capital Medical University, Beijing, China

*** Authors (Lina Li, Jie Gao and Bi-Xi Chen) contributed equally to this work and are co-first authors**

Corresponding authors

Boqia Xie, MD

Cardiac Center, Beijing Chaoyang Hospital, Capital Medical University, 8th Gongtinanlu Rd, Beijing 100020, China

Tel: +86-10-85231400

Email: dr.boqiaxie@hotmail.com

ORCID ID: 0000-0003-4490-9032

Min-Fu Yang, MD

Department of Nuclear Medicine, Beijing Chaoyang Hospital, Capital Medical University, 8th Gongtinanlu Rd, Beijing 100020, China

Tel: +86-10-85231356

Email: minfuyang@126.com

ORCID ID: 0000-0002-9015-0541

Pixiong Su, **MD**

Cardiac Center, Beijing Chaoyang Hospital, Capital Medical University, 8th Gongtinanlu Rd, Beijing 100020, China

Tel: +86-10-85231146

Email: supixiong1130@163.com

Total words:4164 **Tables**: 3 **Figures**: 4

Running title: FAPI imaging in AF

Abstract

Purpose: Radiolabeled fibroblast activation protein inhibitor (FAPI) imaging has proven feasible in the assessment of ventricular fibrosis in several cardiovascular diseases. However, its value in assessing atrial fibrosis in atrial fibrillation (AF) remains unknown.

Methods: Twenty-eight patients with AF and 25 sex-matched controls underwent baseline FAPI PET/CT imaging. Left atrial appendage (LAA) specimens were obtained from seven patients and two lung transplant donors. Atrial pacing beagle dog AF models were constructed by pacemaker implantation. After 8 weeks of pacing, the animals underwent FAPI PET/CT imaging and specimens from the left atrial and right atrial (LA, RA) were collected. FAPI activities in the LA, RA, and LAA were measured by target-to-background ratio (TBR), and the mRNA and protein expression of fibroblast activation protein (FAP) and collagen I were measured by quantitative polymerase chain reaction (PCR) and western blot.

Results: FAPI imaging identified increased atrial uptake in 17 patients with persistent AF (PsAF) (85.00%) and 5 with paroxysmal AF (PAF) (62.50%), located in the LA (64.28%), RA (57.14%), and LAA (42.86%). In all atrial structures, patients with PsAF had a higher prevalence of enhanced FAPI uptake than those with PAF (63.33% vs. 33.33%, $P = 0.02$). LA dilation and B-type natriuretic peptide level were determined as independent factors for increased LAA and RA FAPI uptake, respectively (OR: 1.11 and 1.02, both $P < 0.05$). All five beagles with AF had increased FAPI uptake in the LA and RA. For both human and animal specimens, FAPI activity was strongly associated with the mRNA and protein levels of FAP, and was closely related to the mRNA expression of collagen I.

Conclusion: This preliminary study suggests that FAPI imaging is feasible for assessing activated fibroblasts in the atriums of AF.

Keywords: Fibroblast activation protein inhibitor; atrial fibrillation; atrial fibrosis; fibroblast

Introduction

Atrial fibrillation (AF), which has a diverse pathophysiological background, is the most common arrhythmia in humans [1]. As a progressive disease, in AF, the atrium undergoes structural, contractile, and electrical remodeling, with atrial fibrosis as the hallmark. Studies have proven that atrial fibrosis is involved in the occurrence, maintenance, and recurrence of AF, and is associated with an increased risk of stroke and heart failure [2]. Therefore, proper assessment of atrial fibrosis is necessary for risk stratification and improved treatment.

Late gadolinium enhancement (LGE) magnetic resonance imaging (MRI) has emerged to evaluate atrial fibrosis [3]. However, its application is restricted to certain centers and the reproducibility is unsatisfied due to the absence of standardized image protocols. Moreover, as LGE is limited to the detection of irreversible fibrosis, this technique cannot provide fibrotic information in the initial adaptive phase of atrial remodeling.

The fibrotic process is initiated by the activation of fibroblasts, which specifically express a membrane-anchored peptidase-fibroblast activation protein (FAP). Recently, radiolabeled fibroblast activation protein inhibitor (FAPI)-targeting tracers have been developed to detect activated fibroblasts [4]. Both our research and that of other groups have demonstrated that FAPI imaging is feasible for the assessment of pathological fibroblast activation in ventricles [5,6]. If this technique is also feasible in the atriums, the initial reversible phase of atrial fibrosis could be detected, thus guiding treatments aimed at reversing the pathological fibrotic process. However, no previous study has explored the feasibility of FAPI imaging in the atriums in the context of AF.

Therefore, in this preliminary study, we elucidated the feasibility of FAPI positron emission tomography and computed tomography (PET/CT) imaging for the evaluation of activated fibroblasts in the atriums of AF, with histological evidence.

Materials and methods

Study population

This prospective study was approved by the Institutional Ethical Committee of Beijing Chaoyang Hospital (2021-ke-42) and was conducted in agreement with the Declaration of Helsinki. Patients with persistent AF (n = 20) (PsAF; episode lasting > 7 days) and paroxysmal AF (n = 8) (PAF; episode self-terminated within 7 days) who were treated at the Cardiac Center of Beijing Chaoyang Hospital from February 2021 to March 2022, were prospectively enrolled (20 men, mean age: 61 ± 13 years). A control group of 25 sex-matched healthy volunteers (14 men, mean age: 42 ± 16 years) were recruited to establish the normal range of FAPI activity following the same PET/CT imaging procedures as those used for patients with AF. The inclusion criteria were as follows: no history of AF or other arrhythmias, no history of cardiovascular disease, no history of malignancy, and no abnormal findings on PET/CT imaging. Informed consent was obtained from all subjects.

The left atrial appendage (LAA) samples were obtained from seven patients with PsAF who underwent hybrid surgical-catheter ablation, and from two lung transplant donors with no evidence of cardiac dysfunction.

FAPI image acquisition and interpretation

$Al^{18}F$-NOTA-FAPI was radiolabeled as previously described [7], and PET/CT images were acquired 60 min after injection (2.5–3.0 MBq/kg) using a 16-slice PET/CT scanner (Discovery STE, GE, USA). The CT parameters were as follows: 140 kV; 120 mA; pitch, 1.375;

collimation, 16 × 0.625 mm; and section width, 5 mm. The PET parameters were as follows: two beds of PET images (5 min/bed, 3D mode) with the heart in the center of the view. Attenuation-corrected PET images (voxel size: 3.9 × 3.9 × 3.3 mm) were reconstructed from the CT data using a 3D ordered-subset expectation-maximization algorithm (14 subsets, 2 iterations). Integrated PET and CT images were obtained automatically on AW VolumeShare 2 (GE Healthcare).

The FAPI activity in different atrial structures was analyzed using a quantitative method described previously [8]. In brief, visible uptake of the atrial wall on each PET trans-axial image was measured by placing regions of interest (ROI) under the guidance of CT. The maximum standardized uptake value (SUVmax) of all slices was selected to represent the activity of the atrium. If no visible uptake was observed, a circular ROI of 5 mm in diameter was placed on the right lateral wall of the left atrium (LA) at the level of the right inferior pulmonary vein and the right lateral wall of the right atrium (RA) at the level of the aortic root. The activity of the left atrial appendage (LAA) was obtained by placing an ROI around it on trans-axial sections. Similarly, the SUVmax of all of the slices was selected to represent the activity of the LAA. To obtain a background value of FAPI uptake, an ROI was placed on the left and right atrial cavities and the mean SUV (SUVmean) was recorded. Subsequently, a target-to-background ratio (TBR) was calculated for the bilateral atriums and LAA. Values that were 1.96 standard deviations beyond the control mean were considered abnormal.

Echocardiography

Transthoracic echocardiography images were obtained by echocardiologists who were blinded to the FAPI imaging data using a Vivid E95 echocardiographic system (General

Electric Ultrasound, Milwaukee, WI, USA). The LA volume index (LAVi) and RA area were used to assess atrial enlargement.

Beagle dog model of AF

All experiments were approved by the Institutional Ethical Committee of Beijing Chaoyang Hospital (2021-ke-515). The beagle dog model of AF was constructed via rapid atrial pacing (Supplemental Method 1) [9]. In brief, after left lateral thoracotomy, the LAA was exposed and an electrode was fixed at its base for stimulation. The pacemaker (output: 1.5 V, pulse duration: 2.0 ms; Ensen-1ES+1ST, Ensen, Shanghai, China) was set at 600 beats/min. The sham group underwent the same pacemaker implantation procedure but without atrial pacing. The FAPI PET/CT images were collected after 8 weeks. $Al^{18}F$-NOTA-FAPI (3.7 MBq/kg) was administered 1 h before PET/CT (Discovery STE, GE, USA) scanning. After a scout CT acquisition (120 kV, 10 mA) used for heart positioning, CT transmission scanning (140 kV, 120 mA) was performed for attenuation correction and anatomical localization. A PET scan was acquired immediately after CT scanning, and the scanning time was set to 10 min. The LA and RA samples were harvested after PET/CT imaging.

Histological analysis

Immunofluorescence staining of activated fibroblasts was performed in the samples from the LA, RA, and LAA. All samples were fixed with 4% paraformaldehyde overnight. Paraffin sections of the samples were then incubated with FAP antibody (Abcam, ab53066), vimentin antibody (Abcam, ab92547), and α-smooth muscle actin antibody (Abcam, ab7817). The following day, secondary Alexa Fluor–conjugated antibodies diluted in the same carrier solution (1:200) were added to the sections for 1 h at room temperature. The stained sections were collected by a fluorescence microscope. Quantitative polymerase chain reaction (PCR) and western blot were used to evaluate the mRNA and protein levels of FAP and collagen I in the LA, RA, and LAA (Supplemental Methods 2–5).

Statistical analysis

SPSS Statistics (Version 26.0; IBM) was used to perform the statistical analysis. Continuous variables are described as the mean ± SD, or medians with interquartile ranges. Categorical variables are expressed as absolute numbers and percentages. The variables were compared between groups using Student's *t*-test, Mann–Whitney *U* test, chi-squared test, or Fisher's exact test, as appropriate. Pearson or Spearman correlation analysis was conducted to explore the correlations. Univariate and multivariate logistic regression models were employed to explore the relevant factors for increased FAPI uptake in different atrial structures. A P value < 0.05 was considered statistically significant.

Results

Patient characteristics

The baseline characteristics of the patients are presented in Table 1. A total of 28 patients with AF (20 PsAF, 8 PAF; 20 men, mean age: 61 ± 13 years), and 25 sex-matched healthy controls (14 men, mean age: 42 ± 16 years) were prospectively recruited. The patients with PsAF had a larger LA and RA, and lower LVEF compared to those with PAF (all $P < 0.05$). No statistical differences were found in terms of demographics or comorbidities (all $P > 0.05$). Twelve patients underwent hybrid surgical-catheter ablation, 12 patients received radiofrequency catheter ablation, and four patients received anticoagulant therapy.

Atrial FAPI imaging

Atrial FAPI uptake and relative factors in patients with AF

A total of 17 patients with PsAF (85.00%) and five with PAF (62.50%) had increased atrial FAPI uptake, among whom, 22 (78.57%) had more than one atrial structure showing enhanced FAPI activity in the LA (64.28%), RA (57.14%), and LAA (42.86%) (Table 1, Fig. 1a and b). In all atrial structures, patients with PsAF had a significantly higher prevalence of abnormal FAPI uptake than those with PAF (63.33% vs. 33.33%, $P = 0.02$).

We next explored the relevant factors for the increased FAPI uptake in the LA, LAA, and RA (Supplemental Tables 1–3). The univariate and multivariate logistic regression analyses are presented in Table 2. LAVi was independently related to LAA FAPI uptake (odds ratio [OR]: 1.11, 95% confidence interval [CI]: 1.01–1.21, $P = 0.03$), and B-type natriuretic peptide (BNP) yield was associated with enhanced RA FAPI uptake (OR: 1.02, 95% CI: 1.001–1.04, $P = 0.04$). None of the variates presented in Table 1 were found to be independently relevant to increased LA FAPI uptake (Supplemental Table 4).

Beagle model of AF

All five beagles with AF had increased accumulation of FAPI in both the LA and RA, while no atrial FAPI uptake was observed in the sham group (Fig. 1c).

Histological assessment of atrial samples and their relationship with FAPI activity

FAP+ fibroblasts, which were observed in the atrial samples from patients with AF and beagle models with AF, were rare in the control and the sham groups (Fig. 2). Moreover, the mRNA and protein expression of FAP and collagen I were significantly increased in the atrial samples from patients with AF and beagle models with AF (Fig. 3 and 4). The protein level of FAP was highly related to the mRNA expression of collagen I in the LA and LAA (r values:

0.92 and 0.94; both $P < 0.05$), but showed borderline significance in the RA ($r = 0.87$, $P = 0.058$). Correlation analysis demonstrated that FAPI activities in the LA, RA, and LAA were strongly associated with the corresponding mRNA and protein expression of FAP, and were highly related to the mRNA expression of collagen I (Table 3).

Discussion

As the major cells regulating cardiac fibrosis, fibroblasts undergo phenotypic differentiation into the activated type under pathological conditions, which initiate the fibrotic process [10]. Several pathological triggers of AF have been identified, including high-frequency electrical activity, mechanical stress, ischemia, and inflammation [11,12], all of which result in the development of time-dependent atrial fibrotic remodeling.

By targeting the emblem of activated fibroblast, we demonstrate for the first time that FAPI PET/CT can detect increased FAPI activity in the atriums of AF, and show that the atrial activity is strongly related to the tissue-level expression of FAP and collagen I. These findings support that FAPI PET/CT is a histologically reliable imaging modality for the assessment of activated fibroblasts in the atriums of AF. Fibrillar collagen type I is the major component of the cardiac extracellular matrix, accounting for approximately 80% of the total collagen [13]. As collagen I is synthesized by the fibroblasts as pro-collagen, and FAP is the hallmark of activated fibroblasts and the target of the FAPI tracer, a strong relationship observed between FAPI activity and collagen I mRNA expression is to be expected. We found that FAPI activity was unrelated to the protein level of collagen I, which may be explained by the dynamic collagen degradation regulated by procollagenases; this suggests that the atrial fibrotic alterations detected by FAPI imaging are not at the irreversible end-stage, thus providing guidance for the determination of the antifibrotic therapy window and for selecting suitable candidates.

Although almost 90% of AF thrombosis is found in the LAA, few studies have focused on LAA remodeling. Using LGE MRI, Suksaranjit [14] and Delgado [15] reported that LAA fibrosis was correlated with decreased flow rate and increased post-ablation recurrence. More recently, using histological specimens, Ma and colleagues [11] demonstrated that LAA fibrosis was related to the duration of AF and LA enlargement. However, no previous study has explored the direct relationship between imaging and LAA tissues.

LA enlargement was found to be related to LAA FAPI uptake, but not for the LA. Although this agreed with the findings of Ma et al. [11], the underlying mechanisms remain unknown. In this study, a higher prevalence of enhanced atrial FAPI uptake was demonstrated in patients with PsAF, and those with increased LA FAPI uptake had a significantly larger LA. These findings were congruent with the nature of atrial remodeling, reflecting a heavier pathological burden in PsAF and the maladaptive atrium. We propose that the pathophysiological triggers contributing to LA remodeling are the underlying reasons linking LA dilation to LAA FAPI uptake. For example, inflammation is an inducer of fibroblast differentiation and can result in atrial fibrosis and dilation, but due to the lack of involvement of inflammation in statistical analysis, the only identifiable variate is LA enlargement. This presumption also suggests that although no variate included in this study was found to be relevant to LA FAPI uptake, it may be that the underlying pathological factor was not analyzed, such as inflammation.

Our data showed that elevated BNP was related to RA FAPI uptake. According to previous reports [16,17], BNP is correlated with the mean RA pressure and was upregulated in patients with PsAF, and stretching of the atrial wall is a stimulator for fibroblasts. Therefore, we assume that the FAPI uptake in RA reflects the increased atrial stretch and presume that atrial remodeling may also occur in RA under prolonged AF burden.

This preliminary study had several limitations. First, the sample size was small, with only 28 patients with AF enrolled, and only seven patients who had LAA specimens analyzed. Second, relevant factors for LA FAPI uptake were not clarified; thus, more variates should be included based on a larger study population. Third, as follow-up FAPI imaging was not performed, the evolution of atrial FAPI activity in the dynamic atrial remodeling remains unknown. A multicenter cohort study recruiting more patients with AF with repeat FAPI imaging over an extended follow-up period will provide more evidence on the clinical value of atrial FAPI imaging.

Conclusions

This preliminary study suggests that FAPI imaging is a histologically reliable technique for assessing activated fibroblasts in the atriums of AF, which may be useful in the evaluation of atrial remodeling.

References

1. Everett TH 4th, Olgin JE. Atrial fibrosis and the mechanisms of atrial fibrillation. Heart Rhythm. 2007;4:S24-27. https://doi: 10.1016/j.hrthm.2006.12.040.
2. King JB, Azadani PN, Suksaranjit P, et al. Left atrial fibrosis and risk of cerebrovascular and cardiovascular events in patients with atrial fibrillation. J Am Coll Cardiol. 2017;70:1311-1321. https://doi: 10.1016/j.jacc.2017.07.758.
3. Sohns C, Marrouche NF. Atrial fibrillation and cardiac fibrosis. Eur Heart J. 2020;41:1123-1131. https://doi: 10.1093/eurheartj/ehz786.
4. Altmann A, Haberkorn U, Siveke J. The latest developments in imaging of fibroblast activation protein. J Nucl Med. 2021;62:160-167. https://doi: 10.2967/jnumed.120.244806.
5. Xie B, Wang J, Xi XY, et al. Fibroblast activation protein imaging in reperfused ST-elevation myocardial infarction: comparison with cardiac magnetic resonance imaging. Eur J Nucl Med Mol Imaging. 2022;49:2786-2797. https://doi: 10.1007/s00259-021-05674-9.
6. Diekmann J, Koenig T, Thackeray JT, et al. Cardiac fibroblast activation in patients early after acute myocardial infarction: integration with magnetic resonance tissue characterization and subsequent functional outcome. J Nucl Med. 2022. https://doi: 10.2967/jnumed.121.263555.
7. Wang S, Zhou X, Xu X, et al. Clinical translational evaluation of Al^{18}F- NOTA-FAPI for fibroblast activation protein-targeted tumour imaging. Eur J Nucl Med Mol Imag. 2021;48:4259-4271. https:// doi: 10.1007/s00259-021-05470-5.
8. Xie B, Chen BX, Nanna M, et al. ^{18}F-fluorodeoxyglucose positron emission

tomography/computed tomography imaging in atrial fibrillation: a pilot prospective study. Eur Heart J Cardiovasc Imaging. 2021;23:102-112. https:// doi: 10.1093/ehjci/jeab088.

9. Morillo CA, Klein GJ, Jones DL, Guiraudon CM. Chronic rapid atrial pacing. Structural, functional, and electrophysiological characteristics of a newmodel of sustained atrial fibrillation. Circulation. 1995;91:1588-1595. https://doi: 10.1161/01.cir.91.5.1588.
10. D'Urso M, Kurniawan NA. Mechanical and physical regulation of fibroblast-myofibroblast transition: from cellular mechanoresponse to tissue pathology. Front Bioeng Biotechnol. 2020;8:609653. https://doi: 10.3389/fbioe.2020.609653.
11. Ma J, Chen Q, Ma S. Left atrial fibrosis in atrial fibrillation: mechanisms, clinical evaluation and management. J Cell Mol Med. 2021;25:2764-2775. https:// doi: 10.1111/jcmm.16350.
12. Kurose H. Cardiac fibrosis and fibroblasts. Cells. 2021;10:1716. https://doi: 10.3390/cells10071716.
13. McCurdy S, Baicu CF, Heymans S, Bradshaw AD. Cardiac extracellular matrix remodeling: fibrillar collagens and Secreted Protein Acidic and Rich in Cysteine (SPARC). J Mol Cell Cardiol. 2010;48:544-549. https://doi: 10.1016/j.yjmcc.2009.06.018.
14. Suksaranjit P, Marrouche NF, Han FT, et al. Relation of left atrial appendage remodeling by magnetic resonance imaging and outcome of ablation for atrial fibrillation. Am J Cardiol. 2018;122:83-88. https://doi: 10.1016/j.amjcard.2018.03.027.
15. Delgado V, Di Biase L, Leung M, et al. Structure and function of the left atrium and left atrial appendage: af and stroke implications. J Am Coll Cardiol. 2017;70:3157-3172. https://doi: 10.1016/j.jacc.2017.10.063.

16. Tuinenburg AE, Brundel BJ, Van Gelder IC, et al. Gene expression of the natriuretic peptide system in atrial tissue of patients with paroxysmal and persistent atrial fibrillation. J Cardiovasc Electrophysiol. 1999;10:827-835. https://doi: 10.1111/j.1540-8167.1999.tb00263.x.
17. Doyama K, Fukumoto M, Takemura G, et al. Expression and distribution of brain natriuretic peptide in human right atria. J Am Coll Cardiol. 1998;32:1832-1838. https://doi: 10.1016/s0735-1097(98)00494-x.

Statements & Declarations

Funding

This work was supported by National Key Research and Development Program of China (2021YFF0501401, 2021YFF0501400), Capital’ s Funds for Health Improvement and Research (2022-2-2033) and Beijing Hospitals Authority Clinical Medicine Development of Special Funding Support (ZYLX202105).

Competing interests

The authors declare no competing interests.

Author contributions

All authors contributed to the study conception and design. Lina Li and Bi-Xi Chen performed all the experiments, collected, and analyzed the data; Jie Gao, Xingpeng Liu, Liang Shi, and Yanjiang Wang collected the LAA samples; Lina Li, Bi-Xi Chen, Li Wang and Min-Fu Yang analyzed the PET/CT data; Pixiong Su, Min-Fu Yang, and Boqia Xie conceived the study and interpreted the results. All authors contributed to the article’s revision, agreed to its submission, and had full access to original data.

Data availability

The data underlying this article will be shared on reasonable request to the corresponding author.

Ethics approval

All procedures involving human and animals were carried out in accordance with the ethical standards of the institutional and/or national research committee and with the 1964 Helsinki Declaration and its later amendments or comparable ethical standards.

Consent to participate

Informed consent was obtained from all individual participants included in the study.

Consent for publication

Patients signed informed consent regarding publishing their data and photographs.

Table 1 Baseline characteristics

	PsAF (n = 20)	PAF (n = 8)	Control (n = 25)
Age, years	64 ± 9 †	55 ± 17	42 ± 16
Male, n (%)	16 (80.00)	4 (50.00)	14 (56.00)
Body mass index, kg/m^2	26.90 ± 4.30 †	25.35 ± 2.13 †	22.84 ± 3.04
Hypertension, n (%)	13 (65.00)	6 (75.00)	NA
Coronary artery disease, n (%)	9 (45.00)	2 (25.00)	NA
Percutaneous coronary intervention, n (%)	3 (15.00)	0 (0.00)	NA
Peripheral vascular disease, n (%)	1 (5.00)	0 (0.00)	NA
Diabetes mellitus, n (%)	4 (20.00)	3 (37.50)	NA
Stroke, n (%)	6 (30.00)	2 (25.00)	NA
Hyperlipidemia, (%)	11 (55.00)	3 (37.50)	NA
Active smoking, n (%)	7 (35.00)	2 (25.00)	NA
Alcohol, n (%)	9 (45.00)	2 (25.00)	NA
B-type natriuretic peptide, pg/ml	123.90 ± 81.67	88.86 ± 43.07	NA
Echocardiography			
Left ventricular ejection fraction, %	62 ± 7 *	70 ± 5	NA
Left atrium volume index, ml/m^2	37.11 ± 12.61 *	22.51 ± 4.05	NA
Right atrium area, cm^2	22.94 ± 5.87 *	15.61 ± 2.44	NA
FAPI imaging			
increased left atrial uptake, n (%)	14 (70.00) †	4 (50.00) †	0 (0.00)
increased left atrial appendage uptake, n (%)	10 (50.00) †	2 (25.00) †	0 (0.00)
increased right atrial uptake, n (%)	14 (70.00) †*	2 (25.00) †	0 (0.00)
TBR (left atrium)	1.49 ± 0.26 †	1.45 ± 0.31 †	1.08 ± 0.14
TBR (left atrial appendage)	1.28 ± 0.15 †*	1.13 ± 0.17	1.02 ± 0.10
TBR (right atrium)	1.52 ± 0.46 †	1.33 ± 0.51	0.96 ± 0.13

P-value <0.05 compared with PAF*, controls†, and PsAF‡.

PsAF, persistent atrial fibrillation; PAF, paroxysmal atrial fibrillation; TBR, target-to-background ratio.

Table 2 Regression analysis for FAPI uptake in the left atrial appendage and right atrium

Left atrial appendage						
Variables	Univariate			Multivariate		
	OR	95% CI	P value	OR	95% CI	P value
Left atrium volume index	1.11	1.01-1.21	**0.03**	1.11	1.01-1.21	**0.03**
Right atrium area	1.13	0.97-1.31	0.11	0.95	0.75-1.20	0.67
Right atrium						
Variables	Univariate			Multivariate		
	OR	95% CI	P value	OR	95% CI	P value
PsAF	7.00	1.09-45.16	**0.04**	4.58	0.49-42.98	0.18
B-type natriuretic peptide	1.02	1.001-1.04	**0.04**	1.02	1.001-1.04	**0.04**
Increase left atrial uptake	6.07	1.11-33.24	**0.04**	4.31	0.59-31.57	0.15

OR, odd ratio; CI, confidence interval. PsAF, persistent atrial fibrillation.

Table 3 Correlation analysis of FAPI activity with levels of FAP and Collagen I

	FAP				Collagen I	
	mRNA		Protein		mRNA	
	r	p	r	p	r	p
LA	0.97	0.006	0.89	0.04	0.90	0.04
RA	0.98	0.005	0.88	0.047	0.98	0.004
LAA	0.94	0.001	0.78	0.04	0.85	0.014

LA, left atrium; RA, right atrium; LAA, left atrial appendage.

Figure legends

Figure 1 (a) Diverse FAPI uptake patterns in different atrial structures. (b) Representative FAPI uptake in the LA, LAA, and RA of patients with AF and controls. (c) Representative FAPI uptake in the LA and RA of beagle dog AF models and sham.

Figure 2 (a) Masson and immunofluorescence staining of FAP, vimentin, and α-smooth muscle actin proteins in left atrium (LA) and right atrium (RA) sections from beagle dog models of AF. (b) Staining of left atrial appendage (LAA) sections from patients with AF. Activated fibroblasts were observed in patients with AF, but were rare in controls.

Figure 3 The expression of FAP, vimentin, α-SMA, and collagen I was examined by western blot (a, d), quantitative analysis of protein is shown in (b, e). RT-PCR assays to examine the effect of FAP, vimentin, α-SMA, and collagen I in beagle dog models of AF and sham group (c, f).

Figure 4 (a) The expression of FAP, vimentin, α-SMA, and collagen I was examined by western blot, quantitative analysis of protein is shown in (b). (c) RT-PCR assays to examine the effect of FAP, vimentin, α-SMA, and collagen I in AF patients and controls.

Figures

Figure 1

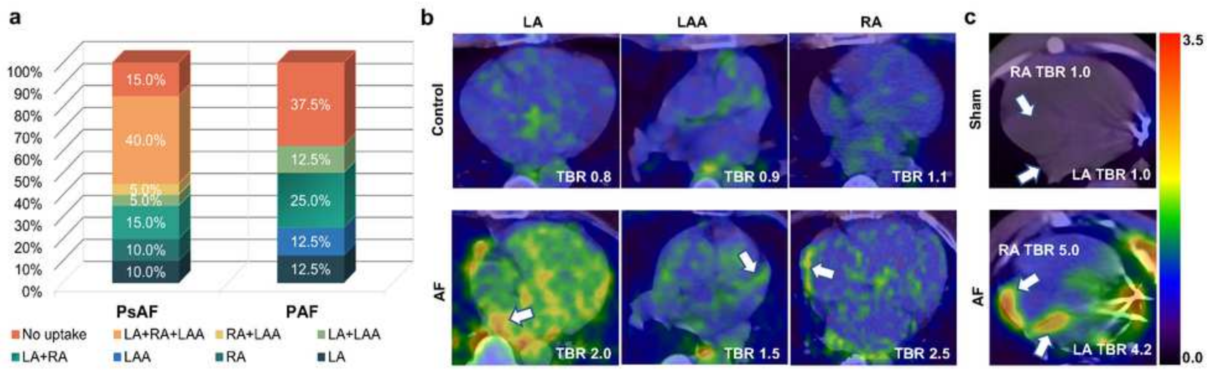

Figure 1

(a) Diverse FAPI uptake patterns in different atrial structures. (b) Representative FAPI uptake in the LA, LAA, and RA of patients with AF and controls. (c) Representative FAPI uptake in the LA and RA of beagle dog AF models and sham.

Figure 2

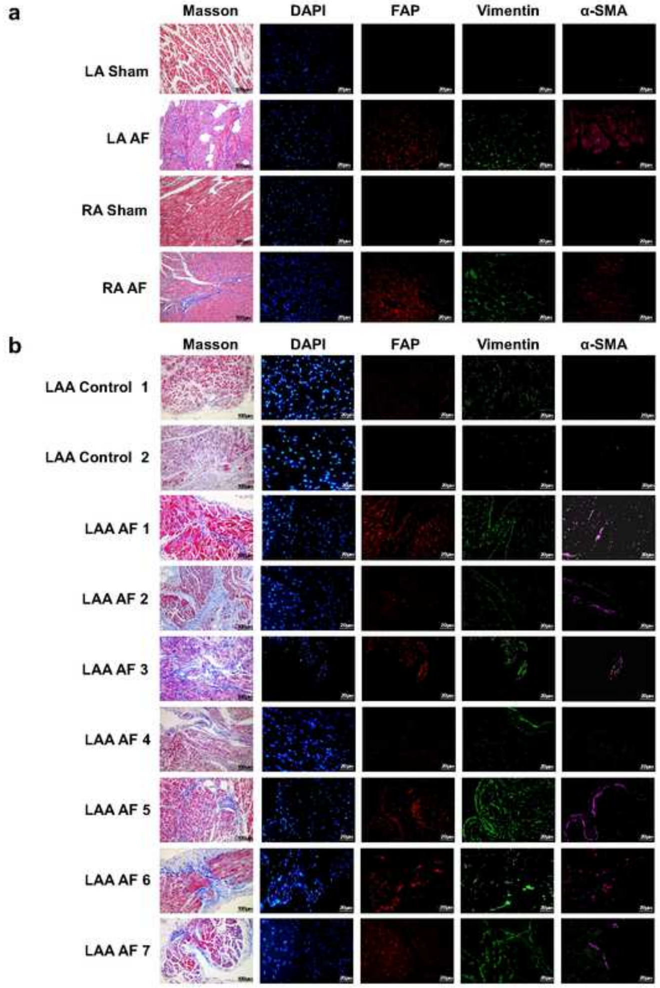

Figure 2

(a) Masson and immunofluorescence staining of FAP, vimentin, and α-smooth muscle actin proteins in left atrium (LA) and right atrium (RA) sections from beagle dog models of AF. (b) Staining of left atrial appendage (LAA) sections from patients with AF. Activated fibroblasts were observed in patients with AF, but were rare in controls.

Figure 3

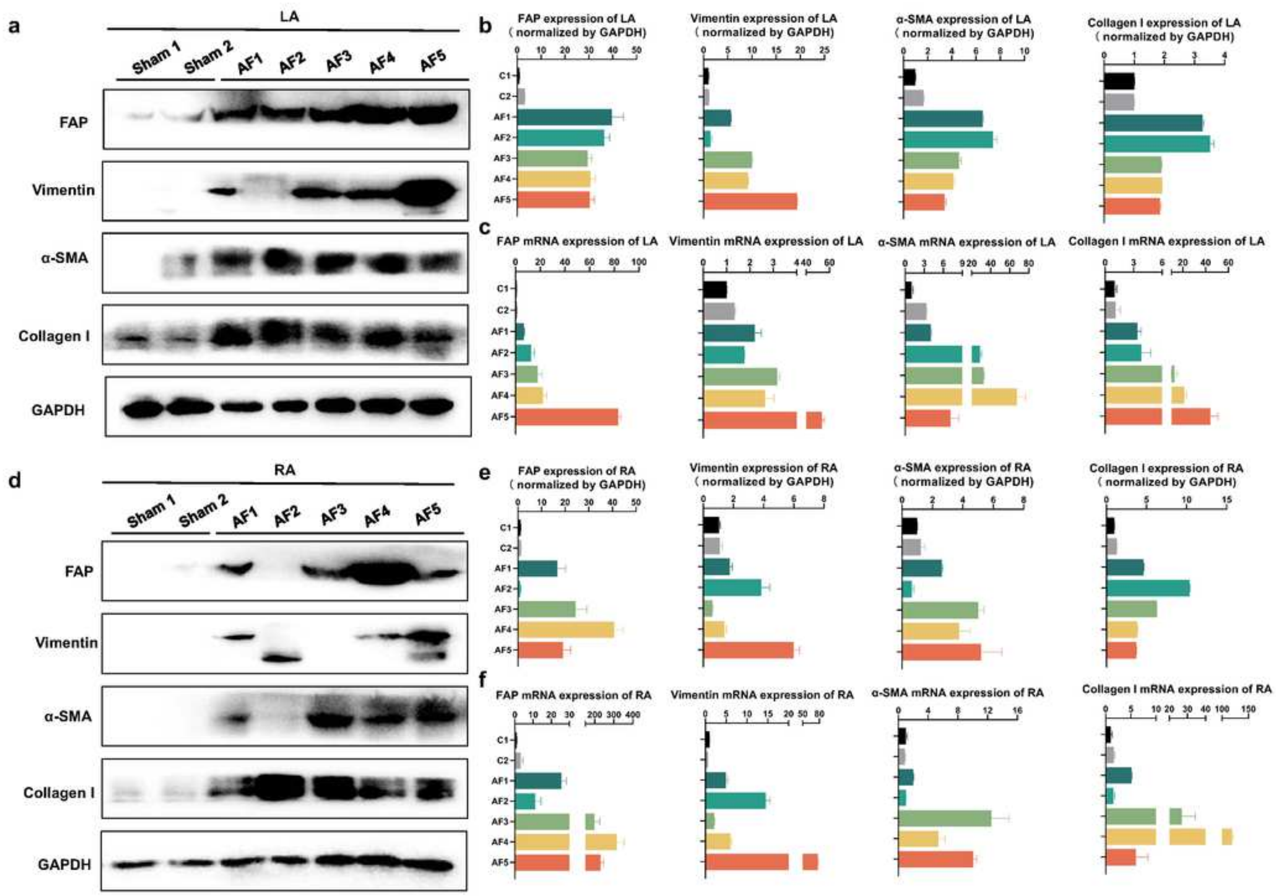

Figure 3

The expression of FAP, vimentin, α-SMA, and collagen I was examined by western blot (a, d), quantitative analysis of protein is shown in (b, e). RT-PCR assays to examine the effect of FAP, vimentin, α-SMA, and collagen I in beagle dog models of AF and sham group (c, f).

Figure 4

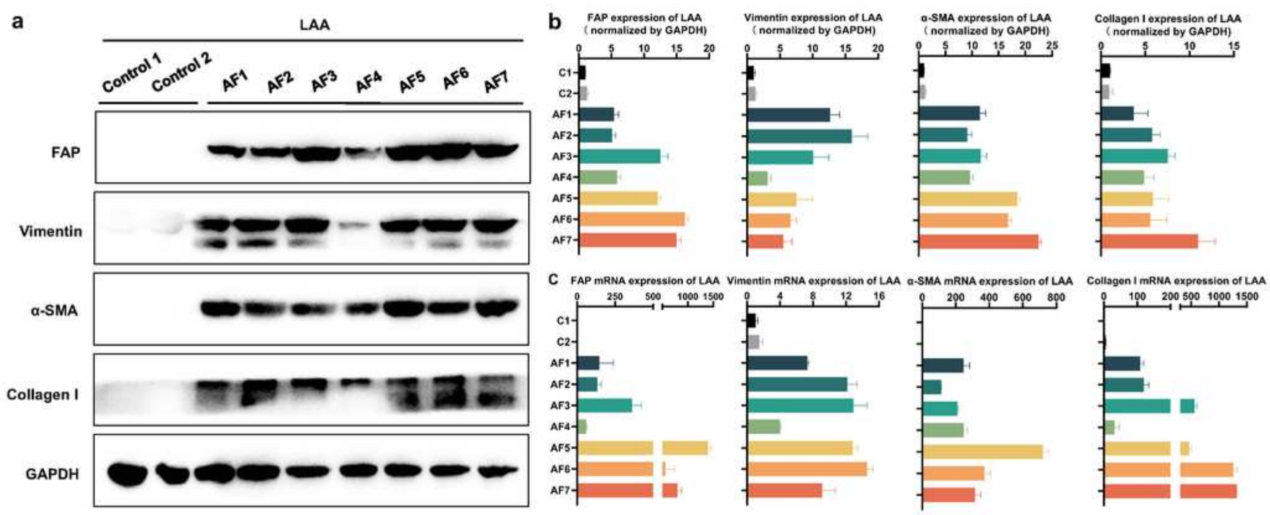

Figure 4

(a) The expression of FAP, vimentin, α-SMA, and collagen I was examined by western blot, quantitative analysis of protein is shown in (b). (c) RT-PCR assays to examine the effect of FAP, vimentin, α-SMA, and collagen I in AF patients and controls.

Supplementary Files

This is a list of supplementary files associated with this preprint. Click to download.

- GA.png
- Supplementmaterial.pdf